



## Provenance groups in a Roman jet jewelry collection at Aquincum (Budapest, Hungary) and comparison with jet and jet-like gemstones

Attila Demény<sup>a,b,\*</sup>, Mária Bondár<sup>c</sup>, Máté Karlik<sup>a,b</sup>, István Hegyi<sup>a,b</sup>, István Gábor Hatvani<sup>a,b</sup>, Annamária R. Facsády<sup>d</sup>, Katalin Csontos<sup>d</sup>, Ariana Gugora<sup>a,b</sup>, Reyhan Kara-Gülbay<sup>e</sup>, Jose Carlos García-Ramos<sup>f</sup>, Sarah Caldwell Steele<sup>g</sup>

<sup>a</sup> Institute for Geological and Geochemical Research, HUN-REN Research Centre for Astronomy and Earth Sciences, Budaörsi út 45, Budapest H-1112, Hungary

<sup>b</sup> CSFK, MTA Centre of Excellence, Konkoly Thege Miklós út 15-17., Budapest H-1121, Hungary

<sup>c</sup> Institute of Archaeology, HUN-REN Research Centre for the Humanities, Tóth Kálmán u. 4., Budapest H-1097, Hungary

<sup>d</sup> Aquincum Museum, Szentendrei út 135., Budapest H-1031, Hungary

<sup>e</sup> Geological Engineering Department, Karadeniz Technical University, Trabzon 61080, Turkey

<sup>f</sup> Museo del Jurásico de Asturias, Rasa de San Telmo, s/n, Colunga 33328, Spain

<sup>g</sup> Department of Archaeology, Durham University, DH1 3LE, United Kingdom

### ARTICLE INFO

#### Keywords:

Jet  
Jewelry  
Roman period  
Fourier Transform Infrared spectroscopy  
Stable hydrogen isotope composition  
Stable carbon isotope compositions  
Hungary

### ABSTRACT

Jet and jet-like gemstones are found in graves from the Neolithic, but they became particularly popular during the Bronze Age and the Roman period. To discover their provenance, several techniques were used to determine distinctions between organic materials and occurrences. The present study utilized a combination of Fourier Transform Infrared spectroscopic (FTIR) and stable isotope ratio analyses to compare a unique Copper Age black bead („Lelle bead”) with Roman period jet items from the Aquincum Museum’s collection and known jet samples from various locations (UK, Spain, Turkey). Visual and multivariate statistical analyses of FTIR spectra, combined with H%, C%, and stable hydrogen and carbon isotope ratio determinations enabled us to distinguish significant ( $p < 0.1$ ) groups among the Aquincum collection: „Lelle-type” samples, „Whitby-type” jets, shales, and coals. Some gemstones were positively identified as Whitby jet, whereas some of the others were indistinguishable from the Lelle bead. This study shows that the coupled FTIR and stable isotope analyses can potentially be used to determine the provenance of archaeological artifacts.

### 1. Introduction

Black, organic gemstones have been found in graves since the Neolithic in Europe. They are scarce in the Chalcolithic (also known as Copper Age) but are common from the Bronze Age and the Roman period (Allason-Jones, 1996; Sheridan et al., 2002; Camaré et al., 2011; Thomas, 2014; Brasser, 2015). The material of these gemstones was called *gagates* by Pliny the Elder, after the district Gagae in Lycia (modern-day Turkey). Jet *sensu stricto* is a type of coalified wood, whose trunks were shed into organic-rich, fine-grained marine sediments during the Jurassic and Cretaceous periods and were coalified and impregnated by bituminous fluids. As a result, the coalified wood pieces became homogeneous. They have conchoidal fractures and can be cut and polished to a high luster, which made it desirable in ancient and modern jewelry. The most important location for true jet is Yorkshire

(UK), where it is found in the Early Jurassic (Toarcian) Mulgrave Shale Member of the Whitby Mudstone Formation (also known as Jet Rock). The most well-known jet occurs in North Yorkshire’s coastal outcrops, but has also been mined extensively inland on the North York Moors. Similar jet occurrences were exploited throughout history in Asturias (NW Spain), the Rhineland (Germany), Languedoc (France), Oltu (Turkey), and Gosau (Austria). Black, organic gemstones may also be produced from lignite, oil shale, and coal, and due to the similar appearance, they are frequently called jet or jet-like gemstones in the literature.

Destructive and non-destructive techniques have been used in attempts to establish a methodology with which to differentiate between materials and locations, i.e., to determine the provenance of the materials. To distinguish jets and shales, Teichmüller (1992) suggested microscopic petrographic analyses; Allason-Jones and Jones (1994),

\* Corresponding author.

E-mail address: [demeny.attila@csfk.org](mailto:demeny.attila@csfk.org) (A. Demény).

<https://doi.org/10.1016/j.jasrep.2024.104413>

Received 30 June 2023; Received in revised form 11 December 2023; Accepted 24 January 2024

Available online 9 February 2024

2352-409X/© 2024 The Author(s). Published by Elsevier Ltd. This is an open access article under the CC BY-NC-ND license (<http://creativecommons.org/licenses/by-nc-nd/4.0/>).

Allason-Jones and Jones (2001) used microscopic techniques (reflectance measurements on polished surfaces); and Hunter et al. (1993) and Sheridan and Davis (1995) applied X-Ray fluorescence (XRF) analysis, whereas Pollard et al. (1981) used neutron activation analysis to determine trace element contents. However, microscopic techniques are problematic because they require a relatively large amount of sample to produce thin sections or representative surfaces. Hand-held XRF analysis is non-destructive, but the variability of most of the elements' concentrations exceeds the differences between jet types (Watts et al., 1997; Brasser, 2015). Fourier Transform Infrared spectroscopy (FTIR) is a tool (Watts and Pollard, 1996) used to effectively distinguish between different organic-rich rocks and coals. With the advent of the attenuated total reflection ATR measurement, FTIR analysis requires only a 1–2 mg sample from the artifact, which can be drilled from areas that will not be visible in future exhibits (e.g., perforation holes of beads). Furthermore, the powder does not need to be mixed with chemical compounds and can be used for other examinations, as well. The powdered sample for FTIR measurements can also be used during the analyses of stable hydrogen and carbon isotope ratios by Isotope Ratio Mass Spectrometry (IRMS), which are another promising method to determine the provenance of coal and amber (e.g., Redding et al., 1980; Mänd et al., 2018).

A combination of XRF, FTIR, and IRMS techniques was used to determine the material characteristics and possible origin of a black organic bead found in a Chalcolithic/Copper Age (approximately mid-4th millennium BCE) grave of a child at Balatonlelle, western Hungary (Bondár et al., 2021). The results of the FTIR and stable isotope analyses led Bondár et al. (2021) suggest that this sample potentially originated from a Carboniferous coal occurrence. The grave also contained copper jewelry, a bead, an armband, and several skulls interred with the child, possibly indicating that the child was of elevated social status. These observations prompted the authors to wonder if the black gemstone derived from a historically significant site that was exploited for millennia to produce jet-like gemstones, or if it originated from an occurrence that was used only by the local populace. Jet jewelry was popular during the Roman period, and the Aquincum Museum (Hungary) possesses an excellent collection (R. Fácásdy, 2009). As such, this study aimed to determine if the material of the jet jewelry collection at Aquincum is similar to that of the Copper Age gemstone. Additionally, samples from known locations containing jet were also analyzed. To distinguish true jet and jet-like materials, the word „jet” will be used to describe the samples derived from the jet locations of Whitby (UK), Asturias (Spain), and Oltu (Turkey) (jet *sensu stricto*), whereas other black organic materials will be called „jet-like” in this paper. The Copper Age gemstone will be termed „Lelle bead”. To compare the FTIR and IRMS results obtained for the Lelle bead with known locations, jet samples from Yorkshire (UK), Asturias (NW Spain), and Oltu (NE Turkey, Kara-Gülbay et al., 2018) were also investigated.

## 2. Materials and methods

### 2.1. Samples

The Lelle bead, the Copper Age black gemstone, was found in a Copper Age grave of an 8–9 year old child (Bondár, 2020; Bondár et al., 2021). The artifact is a flat, oval bead made of a hard material with a shiny surface and is bored through on both sides. It was found at the neck of the 8–9 year old child (Bondár, 2020). The archaeogenetic assessment of the child was undertaken by Bondár and Szécsényi-Nagy (2020). To compare the FTIR and stable isotope results obtained for the Lelle bead with known locations, jet samples from several other locations were also examined. One sample was collected from coastal debris from the northern part of Robin Hood's Bay, south of Whitby (Yorkshire, UK). The strata of the site belong to the Pliensbachian Staithes Sandstone Formation (Korte and Hesselbo, 2011), but being a debris piece, the sample may have originated from the overlying Dogger (Middle Jurassic) strata as well. Although the stratigraphic position is not

constrained, the Robin Hood's Bay sample („RHB”) is included in the investigation as i. the location is a well known jet occurrence (e.g., among collectors in the Victorian era), and ii. jet was also collected by beachcombing during the Roman times for jewelry production (Allason-Jones, 1996), hence it represents an accidental jet piece of beachcombing. One sample, SS1-10, was collected directly from the Mulgrave Shale Member at a horizon 40 cm below the Top Jet Dogger (a tough, calcareous mudstone often used as a roof to support jet mines in the area) by Sarah Caldwell Steele and can be considered a “hard Whitby jet” type specimen. Three samples from Asturias (NW Spain) were collected by Jose Carlos García-Ramos, and eight samples were collected at the Oltu stone site in eastern Turkey by Reyhan Kara-Gülbay. Additionally, a collection of 22 jet-like gemstones (R. Fácásdy, 2009) was sampled and analyzed from the Aquincum Museum. This collection contained necklace beads, armlets, pendants, and hairpins, whose descriptions and photographs are included in the [Supplementary material](#).

### 2.2. Methods

FTIR-ATR measurements were conducted using a Bruker Vertex 70 Fourier Transform Infrared spectroscope equipped with a Platinum ATR accessory. A spectral range of 4000–400  $\text{cm}^{-1}$  was examined, employing a resolution of 4  $\text{cm}^{-1}$ , and a total of 64 scans were recorded per measurement. Each ~3 mg sample was measured 3 times, and the acquired data was evaluated with OPUS 8.1 software.

Multivariate statistical analysis was used to group the FTIR spectra of the jet samples and jet-like gemstones ( $n = 36$ ; [Supplementary Table S1](#); [Figs. 1 and 2](#)). After preprocessing the data (outlier removal, etc.), the FTIR spectra were uniformly trimmed to represent the spectrum between wavenumbers 1800 and 700  $\text{cm}^{-1}$  that contain characteristic peaks. The datasets were then processed using the `pvclust()` function of the `pvclust` package (Suzuki and Shimodaira, 2006) in R (R Core Team, 2023) to obtain groups of similar gemstones with an associated significance level. The  $p$ -values given for hierarchical clustering were obtained through multiscale bootstrap resampling (`nboot = 2000`), allowing for the assessment of the robustness of the clustering results. The chosen significance level used in the study was  $\alpha \approx 0.01$ . Only pairwise complete observations were considered, using Ward's method (`method.hclust = "ward.D"`) with `method.dist = correlation`, i.e., correlation-based clustering. The approach grouped the gemstones based on similar patterns in their FTIR spectra ([Supplementary Material](#)). Spectrum similarity would depend on peak positions on the wavenumber scale, and relative changes in peak intensities (variations in peak ratios). As the measured peak intensities depend on both sample-related and instrument-related factors, Euclidean distance in clustering which would also include absolute intensity values was not applied. Normalization of the individual spectra to their own maximum values and bringing the spectra to the same intensity scale (hence eliminating the measurement effects) is not needed as correlation based clustering is insensitive to linear transformation of the data, i.e., normalization of the spectra. The groupings were determined with and without the Spanish (Asturias) and Turkish (Oltu) samples.

The C concentrations (wt%) and stable carbon isotope compositions of the gemstones were determined using an automated Flash 2000 Elemental Analyzer attached to a Thermo Finnigan Delta V Advantage Isotope Ratio Mass Spectrometer at the Institute for Geological and Geochemical Research (IGGR, Budapest, Hungary). Two-point linear normalization was used to recalculate raw isotope values to VPDB scales, based on analyses of IAEA-CH-6 and IAEA-CH-7 standards.

The hydrogen contents and stable hydrogen isotope compositions of the gemstones were determined using a High Temperature Conversion Elemental Analyzer (TC/EA) attached to a stable isotope ratio measuring mass spectrometer at the IGGR. For bulk analyses, powdered samples were wrapped in Ag foil capsules, placed into a carousel (Uniprep<sup>TM</sup>, Eurovector SpA, Milan, Italy), heated to 110° C, while pumped for 1 h using a Cole Palmer® Air Cadet® diaphragm pump and a liquid

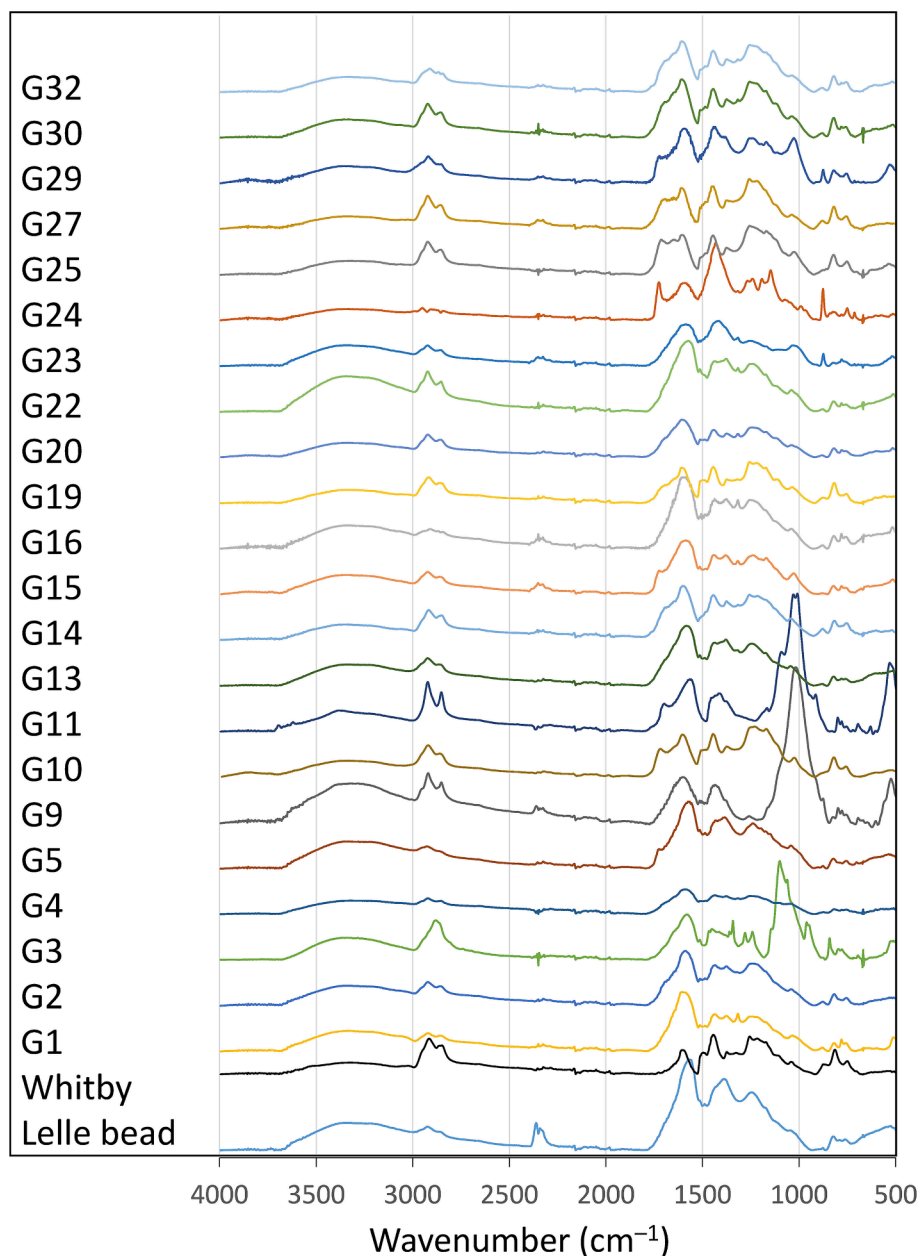


**Fig. 1.** Fourier Transform Infrared spectroscopic spectra of the Whitby jet sample SS1-10, the Lelle bead, and the jet-like gemstone samples from Aquincum (G1 – G32). The vertical axis is not to scale, as spectra are arbitrarily shifted for clarity.

nitrogen trap. To analyze the hydrogen isotope composition of non-exchangeable hydrogen, the protocol in [Wassenaar et al. \(2015\)](#) was followed. The samples were wrapped in Ag foil, placed into the Uni-Prep device, and pumped to vacuum. Then the samples were equilibrated with waters with different isotopic compositions ( $\delta^2\text{H} = -841.3\text{‰}$ ;  $\delta^2\text{H} = -584.3\text{‰}$ ;  $\delta^2\text{H} = -147.7\text{‰}$ ) at  $110\text{ °C}$  for 60 min, after which the water vapor was pumped away. The bulk and equilibrated samples were then flushed with He and dropped into the high-temperature conversion unit (TC/EA) in a continuous flux of He carrier gas. The reaction tube was packed with glassy carbon and heated to  $1430\text{ °C}$ . The TC/EA unit was attached to a Thermo Finnigan delta V mass spectrometer, which was used to determine D/H ratios in the  $\text{H}_2$  gas. The hydrogen contents were calculated based on the size of the mass 2 signal peak.

The isotope compositions were expressed in the  $\delta$  notation ( $\delta^2\text{H}$  and  $\delta^{13}\text{C} = (R_1/R_2 - 1) \cdot 1000$ , where  $R_1$  and  $R_2$  are the  $^2\text{H}/^1\text{H}$  and  $^{13}\text{C}/^{12}\text{C}$  ratios in the sample and the standard, respectively) in permil (‰), relative to V-SMOW for  $\delta^2\text{H}$  and V-PDB for  $\delta^{13}\text{C}$ . The H and C isotope

compositions of laboratory standards (IAEA CH-7 polyethylene foil and NBS-22 oil) used for calibration yielded an average reproducibility of  $< \pm 2\text{‰}$  and  $< \pm 0.1\text{‰}$ , respectively.

### 3. Results and discussion

#### 3.1. Fourier Transform Infrared spectroscopy spectra and their statistical analysis

Altogether, 22 Roman jet-like gemstones from the Aquincum Museum, 1 Copper Age gemstone (Lelle bead), and 13 jet samples – 2 from Yorkshire (UK); 3 from Asturias (Spain); and 8 from Oltu (Turkey) – were analyzed using FTIR, the spectra of which are shown in [Figs. 1 and 2](#) (the spectral data are included in Supplementary [Table 1](#)). As [Fig. 1](#) shows, some groups have similar spectrum patterns (e.g., G3, G9, and G11, with outstanding peaks at around  $1000\text{--}1100\text{ cm}^{-1}$ ). An important goal of this study was to detect samples that may have

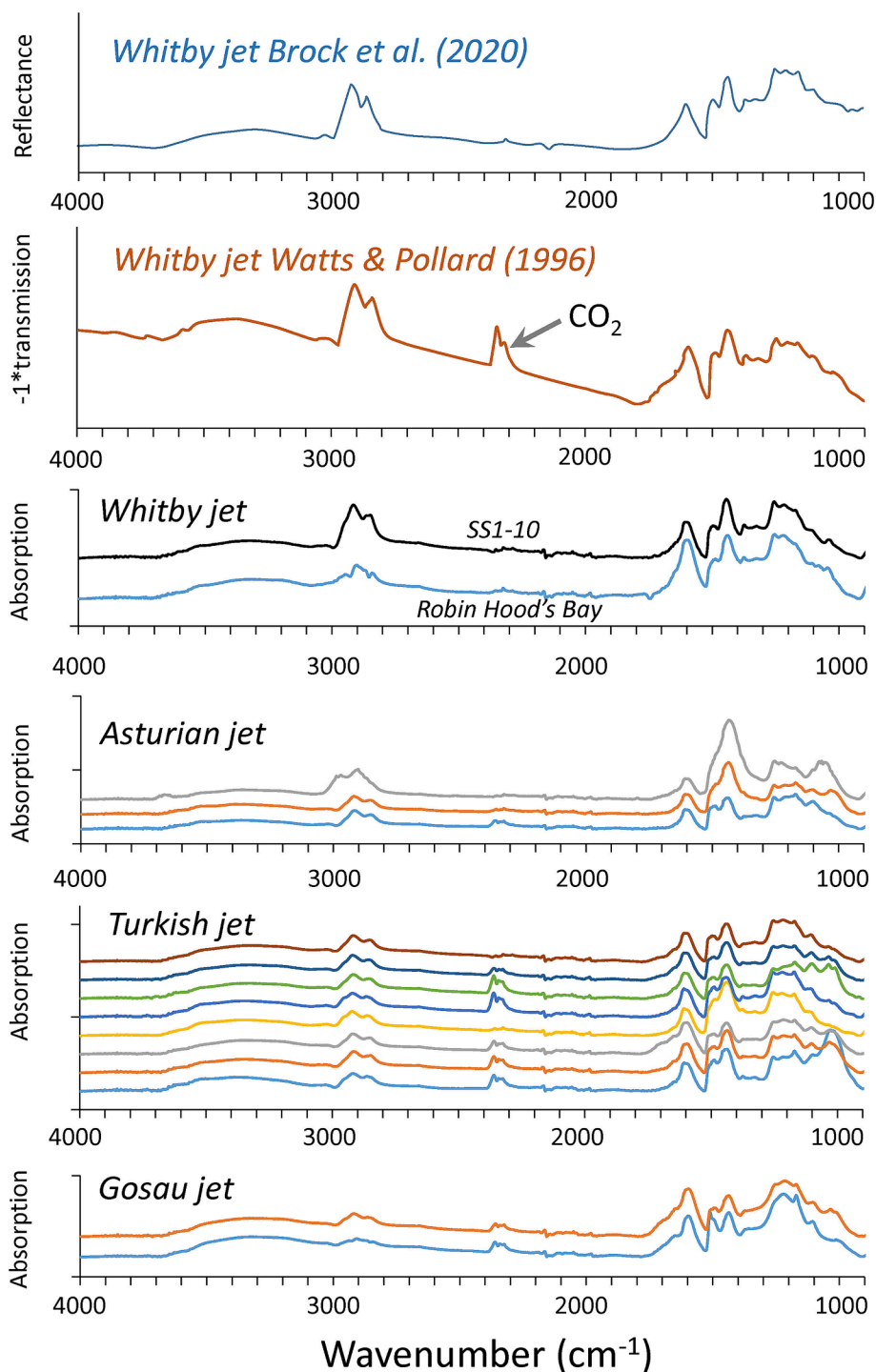


**Fig. 2.** Fourier Transform Infrared spectroscopic spectra of the Whitby jet sample (SS1-10), the Robin Hood's Bay sample, as well as the jet samples from Asturias (Spain), Oltu (Turkey), and Gosau (Austria, from [Bondár et al., 2021](#)). Published spectra for Whitby jets ([Watts and Pollard, 1996](#); [Brock et al., 2020](#)) are shown for comparison. The vertical axes are not to scale, as spectra are arbitrarily shifted for clarity.

originated from the well-known jet occurrence at Whitby (Yorkshire, UK), as such, the Whitby jet spectrum of sample SS1-10 is also shown in [Fig. 1](#). As we have only one sample that can be considered as typical Whitby jet (sample SS1-10), it was also essential to determine if the sample is representative of the Whitby jet site. The FTIR spectra of [Watts and Pollard \(1996\)](#) and [Brock et al. \(2020\)](#) are plotted in [Fig. 2](#). The good agreement of peak positions and intensities suggests that the Whitby jet sample SS1-10 is analogous to the samples analyzed in the cited studies. The jet sample from beachcombing at the Robin Hood's Bay yielded an

FTIR spectrum strikingly similar to the Whitby jet's spectrum. Because jets *sensu stricto* may be formed in other rock strata that were historically exploited for jewelry production, FTIR spectra of samples from other locations (Asturias, Spain; Oltu, Turkey; Gosau, Austria) are also shown in [Fig. 2](#).

The samples can be divided into groups based on visual analyses and selection, but for the sake of objective reproducibility, a multivariate statistical analysis was also conducted on the spectral data. The data were processed with ( $n = 36$ ) and without ( $n = 23$ ) the samples from

**Table 1**

Summary of the classification of samples from the Aquincum Museum based on cluster analysis. Samples belonging to the same groups are significantly different from the other samples ( $\alpha \approx 0.1$ ), according to multiscale bootstrap resampling. The terms “Lelle group”, “Whitby group”, and “Oil shale-type” samples denote the similarity of gemstone samples with the Lelle bead, the Whitby SS1-10 jet, and the oil shales, respectively. The outputs (dendrograms) of the cluster analysis can be found in the Supplementary Material.

	Sample codes
“Lelle group” samples	G1, G2, G4, G5, G13, G15, G16, G22
“Whitby group” samples	G10, G14, G19, G20, G25, G27, G30, G32
“Oil shale”-type samples	G3, G9, G11
Similar to lignites	G23, G24, G29

Asturias (Spain) and Oltu (Turkey). The dendrograms are shown in the [Supplementary Material](#), the main sample groups are listed in [Table 1](#). As expected, the Whitby (sample SS1-10) and the Robin Hood’s Bay jets are close to the Asturian and Turkish jets in the correlation-based dendrogram ([Supplementary Material](#), Section 4A), indicating their similar formations. The Lelle bead is almost identical to sample G5 (rhomboid necklace; *significance*  $\geq 95\%$  [Supplementary Material](#), Sect. 4). Samples G1, G2, G4, G5, G13, G15, G16, G22 can also be classified as within the “Lelle group” ( $\sim 100\%$  significance) in both dendrograms (with or without the Spanish and Turkish jets). Samples G10, G14, G19, G20, G25, G27, G30, G32 can be listed in the “Whitby group” (91 % significance; Supplement 4B, the dendrogram obtained without the Spanish and Turkish jets). In addition to these groups, the dendrograms revealed two separate clusters, consisting of samples G3, G9, and G11 in one and samples G23, G24, and G29 in the other ( $\sim 100\%$  and  $\geq 91\%$  significance respectively). The 700 to 2000  $\text{cm}^{-1}$  section of the FTIR

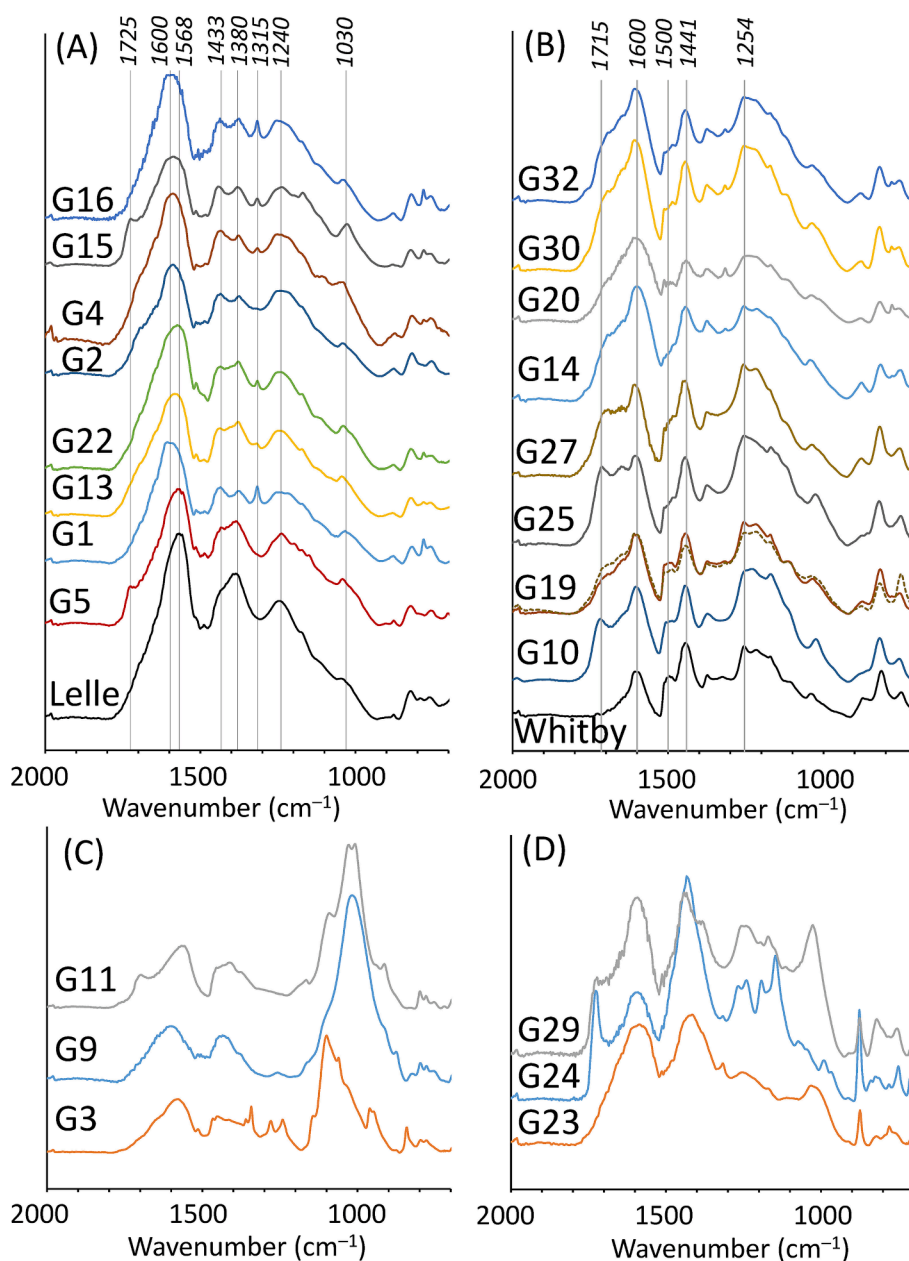


**Fig. 3.** Fourier Transform Infrared spectroscopic spectra of the Whitby jet sample SS1-10, the Lelle bead, and the gemstone samples from Aquincum plotted in groups differentiated using dendrograms (see [Table 1](#)). The vertical axes are not to scale, as spectra are arbitrarily shifted for clarity. Figures A), B), C), and D) show the spectra according to the dendrogram-based groups (see text). The dashed line of sample G19 is the spectrum of the chloroform-treated sample.

spectra is plotted separately using these group divisions in Fig. 3. The spectrum patterns of the „Lelle group” (Fig. 3A) are relatively simple compared to those of the other groups, as the 700 to 2000  $\text{cm}^{-1}$  section is dominated by 3 major peaks at about 1240, 1300, and 1600  $\text{cm}^{-1}$ . Visual inspection indicates that samples G5 and G22 are the most similar to the Lelle bead. The other samples in the Lelle group show slightly different peak ratios at 1380 and 1433  $\text{cm}^{-1}$ , a dominating peak at 1600  $\text{cm}^{-1}$  (in contrast to the 1568  $\text{cm}^{-1}$  peak of the Lelle bead), or the appearance of an additional peak at 1315  $\text{cm}^{-1}$ . The spectra of the „Whitby group” (Fig. 3B) is very different to the „Lelle group” spectra in Fig. 3A. The spectra of the SS1-10 Whitby sample, the Robin Hood’s Bay’s sample, and the G10, G19, G25, and G27 samples are nearly identical in the range of 700 to 1600  $\text{cm}^{-1}$ , whereas the spectra of the G14, G20, G30, and G32 samples differ slightly in peak ratios or due to the appearance of a small peak at 1310  $\text{cm}^{-1}$ . The major difference within the Whitby group is the appearance of the 1715  $\text{cm}^{-1}$  peak, or a hump, at this wavenumber. A possible explanation for this peak is that the gemstones were treated with wax or oil to make the surface shinier (Allason-Jones, 1996), although it is generally applied only to shales. To determine if this was the case, a batch of sample G19 (from which enough powder was available and which showed a hump at 1715  $\text{cm}^{-1}$ ) was treated with chloroform overnight, decanted, dried, and measured. The spectrum of the chloroform-treated sample (dashed line, Fig. 3B) is very similar to that of the untreated sample. As such, this gemstone was likely not treated with oil or wax, so the 1715  $\text{cm}^{-1}$  peak cannot be attributed to the presence of an organic lacquer.

The third group (G3, G9, G11) has additional peaks at 1000–1100  $\text{cm}^{-1}$ , which can be attributed to silicates. The spectra are very similar to that of the oil shales in Penton (2008), thus, they are termed „oil shale”-type. Finally, the group comprising samples G23, G24, and G29 shows spectra that are not similar to any of the other groups’ spectra; they instead resemble the patterns reported for lignites by Cepus et al. (2016).

The Lelle bead and other samples in its group (G5, G13, G22) are characterized by a dominant peak at 1568  $\text{cm}^{-1}$ , slightly shifted from the 1600  $\text{cm}^{-1}$  peak, which is common in coals (e.g., in the other samples in this study, as well as in the coals of Ibarra et al., 1996; Cepus et al., 2016; and Zieger et al., 2020). Similar shifts have been detected by heating coals to 300–400° C (Blanco et al., 1991; Zhang et al., 2015) or by chemically treating coals with amino acids at 70° C (To et al., 2017). This may indicate that the original material of the Lelle bead and some of the other samples in its group derived from coals that had been heated or had undergone exchange with organic-rich fluids. Excluding the shift of the 1600  $\text{cm}^{-1}$  peak, the „Lelle group” spectra are very similar to those of Carboniferous coals found in Spain and France (Iglesias et al., 1995, see also Bondár et al., 2021), as well as in the Ruhr region (Germany) (Zieger et al., 2020). As such, we can be confident that these samples are not true jets (coalified and bitumen-impregnated wood trunks drifted into Jurassic sediments). On the other hand, the strong similarities in the FTIR spectra of the Whitby-group samples with the SS1-10 Whitby jet sample potentially indicate a joint/similar provenance.

In conclusion, FTIR analyses can serve as a fingerprint technique to define groups in a set of samples, as well as to detect similarities and differences when compared with known locations. Additional, independent analyses can further refine the provenance determinations.

### 3.2. D/H ratios in bulk vs. non-exchangeable hydrogen

Organic matter, such as coal, is rich in hydrogen, which makes hydrogen isotope analysis appealing for provenance studies, particularly if combined with other data, like stable carbon isotope compositions (e.g., Redding et al., 1980; Mänd et al., 2018). Potential drawbacks are the mobility of hydrogen and its known sensitivity to late-stage isotope exchange with ambient solutions, which necessitate the analysis of the non-exchangeable hydrogen content (Schimmelmann et al., 1999; Mastalerz and Schimmelmann, 2002). Measuring the hydrogen isotopes

of the non-exchangeable hydrogen content requires a larger sample size. As a result, bulk analyses were conducted for all of the samples, and non-exchangeable hydrogen analyses were performed on the artifacts that contained sufficient sample material. The data are listed in Supplementary Table 2. Excluding one outlier (G13), the  $\delta^2\text{H}$  values of non-exchangeable hydrogen ( $\delta^2\text{H}_{\text{nonex}}$ ) correlate positively with the bulk values ( $\delta^2\text{H}_{\text{bulk}}$ ), with an  $r^2$  value of 0.93, a slope of 1.2, and an average  $\delta^2\text{H}$  bulk-nonex difference of  $-8.8\text{‰}$  ( $\pm 3.7\text{‰}$   $1\sigma$ ). This good agreement may suggest that either 1) late-stage isotope exchange did not significantly affect the hydrogen content, so the bulk  $\delta^2\text{H}$  data may be used in provenance analysis, or 2) even the „non-exchangeable” hydrogen has been altered. Comparison with additional data is needed to determine which of the two conclusions is valid.

### 3.3. H-C contents and stable isotope compositions

Hydrogen and carbon contents (H% and C% values), as well as stable hydrogen and carbon isotope compositions are listed in Supplementary Table S2 and are plotted in Fig. 4, with the FTIR-based groups specified. The H% and C% values (Fig. 4A) clearly define three major fields. The Asturian, and the Turkish jet samples plot within a small area, indicating that they formed in similar environments and under similar processes. Sample SS1-10, which is considered to be representative of Whitby gemstones, yielded relatively high H% and C% values, which are nevertheless close to the Turkish and Asturian jet fields. The Robin Hood’s Bay sample (RHB) plots within the jet field close to the Asturian samples. The „Whitby group” samples plot close to the jet field, partly overlapping it, and the G19 sample is very close to the SS1-10 sample. The values of the Lelle bead fall between those of samples G5 and G22, which have the most similar FTIR spectra to that of the Lelle bead. The „Lelle group” (Fig. 3A and Table 1) shows a large scatter and overlaps with the oil shale-like samples, as well as with the non-classified samples (Fig. 3C and D).

The C contents and carbon isotope compositions are generally less sensitive to late-stage alteration, and the incorporation of secondary carbonate (which would affect both variables) was not detected by FTIR. The jet samples plot close to each other in Fig. 4B, although the Turkish jets appear to have higher C% and  $\delta^{13}\text{C}$  values than the Asturian ones, and the SS1-10 Whitby sample is shifted to higher C% values. The RHB sample plots in the middle of the jet field. Among the Whitby group gemstones sample G19 plots closest to the jet field. The „Whitby group” samples, however, plot away from the jets, with more negative  $\delta^{13}\text{C}$  and slightly lower C% values. As for the „Lelle group”, sample G2 plots close to the jet field, whereas G13 and G15 have low  $\delta^{13}\text{C}$  values that are similar to the low end of the „Whitby group” field. Although the FTIR spectrum of G4 is within that of the „Lelle group” (Fig. 3A), the low H and C contents (Fig. 4A and B) make it an outlier. The C% and  $\delta^{13}\text{C}$  values of the Lelle bead and sample G5 are very close to each other, nearly within the analytical precision.

The H%- $\delta^2\text{H}$  plot (Fig. 4C) reveals systematic data distributions. The Lelle bead is an outlier, with a relatively low  $\delta^2\text{H}$  value, which may be

**Table 2**

Comparison of the classifications in Allason-Jones and Jones (2001) and this study. Vitrinite reflectance data (%RO) from Allason-Jones and Jones (2001) are also listed.

Samples of this study	Classification of this study	Classification of A-J & J	%RO
G1	„Lelle group”	jet (pendant AM.1993)	0.18
G3	„oil shale”-type	jet (beaded armlet AM.632a and b)	0.1–0.14
G11	„oil shale”-type	shale (armlet AM.70.6.79 Unpubl.)	0.35
G19	„Whitby group”	jet (armlet AM51468)	0.17
G23	similar to lignite	jet (beaded armlet AM52379)	0.23

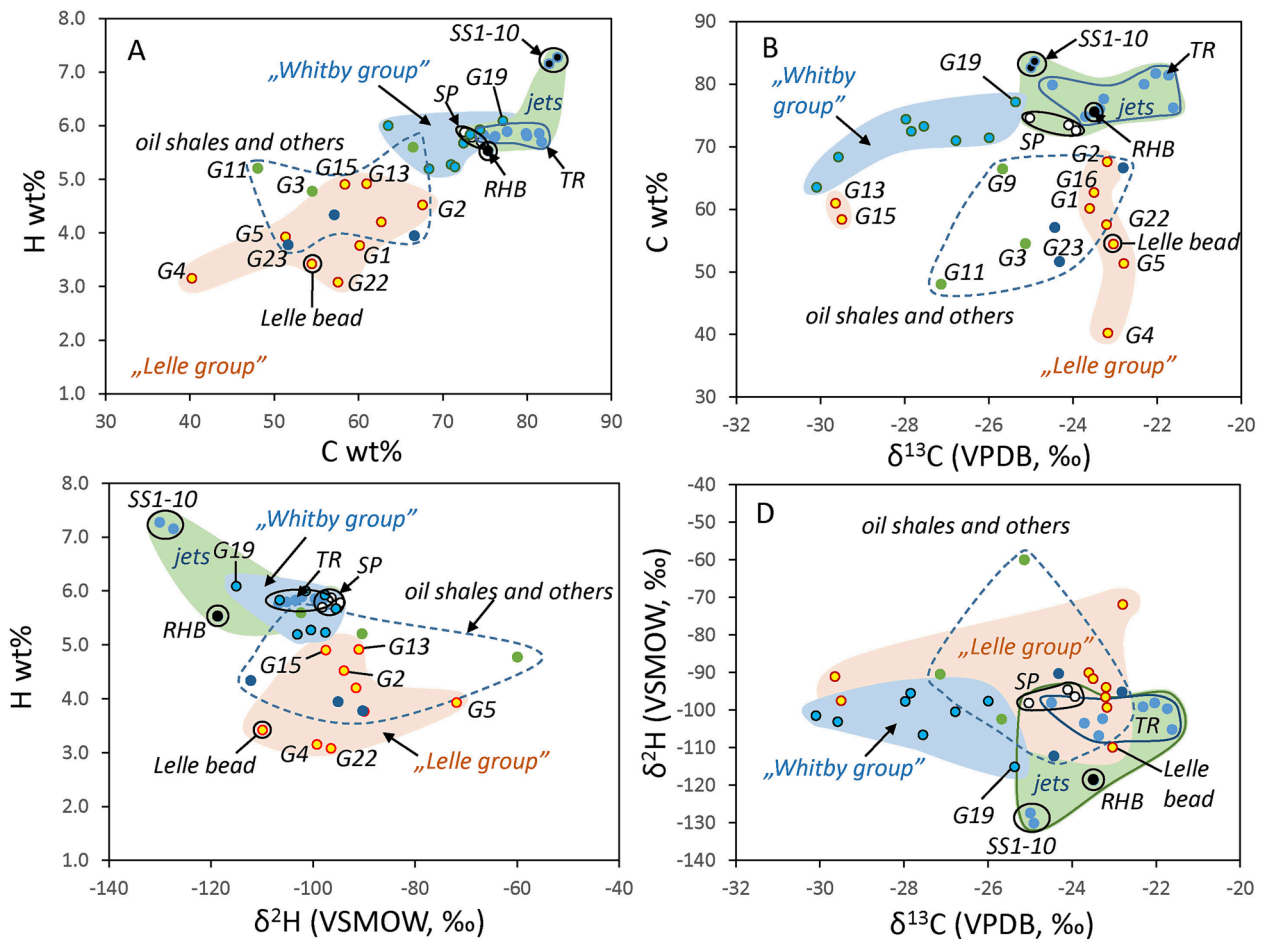


**Fig. 4.** Hydrogen and carbon contents (H% and C% in wt%), as well as stable hydrogen and carbon isotope compositions (in ‰ relative to VSMOW and VPDB, respectively) of the studied samples. Data groups follow the dendrogram-based division (see Table 1). Jet samples from Asturias are marked by white, filled circles within the jet fields. RHB: Robin Hood's Bay sample. SS1-10: Whitby jet sample. TR and SP: samples from Turkey and Spain, respectively.

related to postdepositional alteration in the grave's soil where the bead was found. The Asturian and the Turkish jets overlap with the „Whitby group” samples, whereas the SS1-10 Whitby and the RHB samples are characterized by lower  $\delta^2\text{H}$  values. Interestingly, the SS1-10 Whitby sample is shifted from the other jets due to its elevated H%, whereas the RHB sample plots close to the Asturian and Turkish jets and the „Whitby-group” samples. Sample G19 again plots closest to the Whitby sample compared to other Whitby group gemstones. The H% and  $\delta^2\text{H}$  values clearly separate the „Whitby group” samples from the „Lelle group”-objects. Samples G2, G13, and G15 are again closest to the jet field, as depicted in Fig. 4A and 4B. The combined  $\delta^2\text{H}$ - $\delta^{13}\text{C}$  diagram shows overlapping compositions, without revealing new relationships.

These data distributions show that provenance investigations using FTIR and stable isotope analyses are not straightforward but that diagnostic features may nevertheless be inferred. The good separation of the „Whitby group” and the „Lelle group” samples in the H%- $\delta^2\text{H}$  results indicates that bulk hydrogen measurements may be helpful in provenance research and that the compositions of exchangeable hydrogen are not shifted from the formation-related values. The non-exchangeable H% and  $\delta^2\text{H}$  values are not discussed here, as their quantity of data is smaller than that of the bulk analyses. The H% and C% values clearly differentiate between jet and non-jet samples. The latter may be derived from coal deposits. The similarities in the FTIR spectrum and the previously published  $\delta^{13}\text{C}$  ranges (Redding et al., 1980; Iglesias et al., 1995; Bondár et al., 2021) suggest that the most likely origin for the Lelle bead, as well as for samples G1, G5, G16, and G22 is Carboniferous coal. As for the jet-like samples, only one sample's (G19) material is

similar to the SS1-10 Whitby or the RHB samples. The other FTIR-based „Whitby-group” samples may originate from related jet occurrences, but they are not similar to the Robin Hood's Bay sample or the SS1-10 sample. Although the age and formation of the Kimmeridge jet (another jet occurrence in the UK also used for black jewelry, Watts and Pollard, 1996) are similar to those of the Whitby jet, the Kimmeridge jet has a slightly different FTIR spectrum (Watts and Pollard, 1996). Therefore, the „Whitby group” samples may not originate from this formation type. Hesselbo et al. (2007) analyzed stable carbon isotope compositions of jet samples from the Early Jurassic Mulgrave Shale Member (Yorkshire, UK). Their  $\delta^{13}\text{C}$  values range from  $-30.8$  to  $-24.7$  ‰, with a systematic stratigraphic variation („negative carbon isotope excursion”). As such, the  $\delta^{13}\text{C}$  range of  $-30$  to  $-25$  ‰ of the „Whitby group” samples may be consistent with an origin from Yorkshire jet occurrences. Based on the  $\delta^{13}\text{C}$  value of  $-25$  ‰, sample SS1-10 may be correlated with the wood compositions detected at layers 39 and 40 in the sedimentary section of Hawsker Bottoms (Yorkshire, UK) in Hesselbo et al. (2000). The  $\delta^{13}\text{C}$  value of  $-23.5$  ‰ of the Robin Hood's Bay sample is unusually high compared to the Toarcian jet range of Hesselbo et al. (2000), but would be consistent either with Pliensbachian wood compositions observed for the Robin Hood's Bay sedimentary section ( $\delta^{13}\text{C}$  values mainly between  $-26$  and  $-23$  ‰; Korte and Hesselbo, 2011), or with middle Jurassic wood  $\delta^{13}\text{C}$  data of the Ravenscar Group, Yorkshire (from  $-26$  to  $-21$  ‰, Hesselbo et al., 2003). The FTIR, chemical, and stable isotope similarities of the G19 gemstone with the SS1-10 and RHB samples indicate that the G19 material may have derived from a source which is identical to the “hard jet” of Whitby or the “soft jet” of

the Robin Hood's Bay. The similar FTIR spectra but different isotopic compositions of the jets and the "Whitby group" gemstones, as well as the overlapping  $\delta^{13}\text{C}$  ranges of the "Whitby group" gemstones ( $-30.1$  to  $-25.4$  ‰) and the Hesselbo et al. (2007) jet range ( $-30.8$  to  $-24.7$  ‰) indicate that the materials for the "Whitby group" gemstones may have been collected from different stratigraphic positions within the lower Jurassic jet-bearing layers. Further detailed sampling of the potential jet mining locations, as well as of Roman jewelry from Yorkshire may shed light on the provenance of Roman jet artifacts.

#### 4. Comparison with microscopic reflectance studies

Some of the samples from the Aquincum Museum collection (marked „AM") were studied using reflected light microscopy and were classified as jets and shales by Allason-Jones and Jones (2001). Table 2 shows the comparison of the two studies. Out of the 5 samples analyzed in both studies, only 2 identifications matched (samples G11 and G19). Three other samples were identified as jets by Allason-Jones and Jones (2001), but they plotted outside of the jet fields in Fig. 4 and were classified as „Lelle group" (sample G1), „oil shale"-type (sample G3), and lignite-like (sample G23). As suggested by Bondár et al. (2021), the FTIR and geochemical characteristics of the Lelle bead are similar to those of Carboniferous coal. This is in accordance with the low H% and C% values of the „Lelle group" samples, which are characteristic of coal rather than jets (Pollard et al., 1981). Textural characteristics would help to determine the material type (e.g., Teichmüller, 1992), but our results show that reflectance alone may not be sufficient to distinguish between jets and other coal-like materials. Textural analysis by a reflected light microscope, however, requires a large piece of the sample to be cut and polished, whereas the powder sampling used for the coupled FTIR-IRMS requires only a small amount of material (1–2 mg), which can be taken without damaging the artifact for future museum exhibits.

#### 5. Conclusions

Black, organic gemstones from a Copper Age grave at Balatonlelle (western Hungary) and from the Aquincum Museum's Roman period collection (Budapest, Hungary), as well as jet samples from Yorkshire (UK), Asturias (NW Spain), and Oltu (Turkey) were investigated using Fourier Transform Infrared (FTIR) spectroscopy, H and C concentrations, and stable isotope ratio determinations. The FTIR spectra were statistically processed and grouped using correlation-based metrics, accompanied by bootstrapping. Four major groups were differentiated: 1) samples similar to the Copper Age Lelle bead, 2) samples similar to Whitby jet, 3) samples with spectrum patterns similar to oil shales, and 4) non-classified samples that may be similar to coals. The H-C contents and stable isotope compositions also helped to refine the sample groups. Combining the FTIR, chemical, and isotopic information, some of the Aquincum samples were nearly identical to the Lelle bead, one sample was very similar in all aspects to the Whitby jet sample, and seven gemstones had Whitby-like FTIR spectra but a  $\delta^{13}\text{C}$  range that overlapped published  $\delta^{13}\text{C}$  values of lower Jurassic wood from Yorkshire (UK). This observation warrants further, systematic study on the provenance of Roman jet jewelry and stratigraphically well-known jet occurrences. Additional samples may represent oil shales and lignite-like coal on the basis of their FTIR spectra and chemical compositions. Although exact origins cannot be conclusively determined, this study demonstrates that combined geochemical analyses are potentially useful in future provenance research.

#### CRedit authorship contribution statement

**Attila Demény:** Conceptualization, Data curation, Formal analysis, Investigation, Supervision, Writing – original draft, Writing – review & editing. **Mária Bondár:** Formal analysis, Investigation. **Máté Karlik:** Data curation, Formal analysis, Investigation, Methodology. **István**

**Hegyí:** Data curation, Formal analysis, Investigation, Methodology. **István Gábor Hatvani:** Data curation, Formal analysis, Investigation, Methodology. **Annamária R. Facsády:** Formal analysis, Investigation. **Katalin Csontos:** Formal analysis, Investigation. **Ariana Gugora:** Conceptualization, Formal analysis, Investigation, Writing – original draft, Writing – review & editing. **Reyhan Kara-Gülbay:** Investigation. **Jose Carlos García-Ramos:** Investigation. **Sarah Caldwell Steele:** Investigation.

#### Declaration of Competing Interest

The authors declare that they have no known competing financial interests or personal relationships that could have appeared to influence the work reported in this paper.

#### Data availability

The data will be published in Supplementary Tables.

#### Acknowledgements

This study was undertaken as part of the research project "Complex analysis of the Late Copper Age burials of the Carpathian Basin", funded by a grant from the National Research Development and Innovation Office Fund of Hungary (Project NKFI-K-128413, PI: Mária Bondár). Professor Steve Hesselbo and an anonymous reviewer provided constructive and helpful review that helped improve the paper.

#### Appendix A. Supplementary data

Supplementary data to this article can be found online at <https://doi.org/10.1016/j.jasrep.2024.104413>.

#### References

- Allason-Jones, L., 1996. Roman jet in the Yorkshire Museum. *Yorkshire Museum* 55.
- Allason-Jones and Jones, 1994. Jet and other materials in Roman artefact studies. *Archaeologia Aeliana* 5, 265–272.
- Allason-Jones, L., Jones, J.M., 2001. Identification of 'jet' artefacts by reflected light microscopy. *European Journal of Archaeology* 4, 233–251.
- Blanco, C., Fdez Ferreras, J., Pajares, J.A., Mahamut, M., Pérez, A., Pis, J.J., 1991. Characterization of a Spanish Coal and Study of the Influence of Oxidation Time by Ftirs. *Spectroscopy Letters* 24, 827–836. <https://doi.org/10.1080/00387019108018162>.
- Bondár, M., 2020. Késő rézkori különleges temetkezések Balatonlelléről (Somogy m.) – Unusual burials of the Late Copper Age at Balatonlelle (County Somogy, Hungary). *A Kaposvári Rippl-Rónai Múzeum Közleményei* 7, 89–105.
- Bondár, M., Szécsényi-Nagy, A., 2020. Skull cult in the Late Copper Age. *Ziridava* 34, 91–104.
- Bondár, M., Demény, A., Németh, P., Karlik, M., Fintor, K., ŐTóth, ?, 2021. Különleges gyöngy egy különleges késő rézkori sírból. – Special bead from a special Late Copper Age Grave. *Archeometriai Műhely XVIII/2*, 143–156.
- Brasser, J.P., 2015. Jet artifacts from two Neolithic sites on the Dutch coast: An experimental approach. Master of Science, Material Culture Studies Leiden University, Faculty of Archaeology, Thesis. Leiden., p. 106
- Brock, F., Ostapkowicz, J., Collinson, M.E., Bull, I.D., Dyer, C., Lane, D.W., Domoney, K., Uden, J., 2020. Dark materials: Pre-Columbian black lithic carvings from St Vincent and the wider Caribbean. *Journal of Archaeological Science: Reports* 32, 102393.
- Cepus, V., Borth, M., Seitz, M., 2016. (2016): IR Spectroscopic Characterization of Lignite as a Tool to Predict the Product Range of Catalytic Decomposition. *International Journal of Clean Coal and Energy* 5, 13–22.
- Hesselbo, S.P., Gröcke, D.R., Jenkyns, H.C., Bjerrum, C.J., Farrimond, P., Bell, H.S.M., Green, O.R., 2000. Massive dissociation of gas hydrate during a Jurassic oceanic anoxic event. *Nature* 406, 392–395.
- Hesselbo, S.P., Morgans-Bell, H.S., McElwain, J.C., Rees, P.M., Robinson, S.A., Ross, C.E., 2003. Carbon-Cycle Perturbation in the Middle Jurassic and Accompanying Changes in the Terrestrial Paleoenvironment. *The Journal of Geology* 111, 259–276.
- Hesselbo, S.P., Jenkyns, H.C., Duarte, L.V., Oliveira, L.C.V., 2007. Carbon-isotope record of the Early Jurassic (Toarcian) Oceanic Anoxic Event from fossil wood and marine carbonate (Lusitanian Basin, Portugal). *Earth and Planetary Science Letters* 253, 455–470.
- Hunter, F.J., McDonell, J.G., Pollard, A.M., Morris, C.R., Rowlands, C.C., 1993. The scientific identification of archaeological jet-like artefacts. *Archaeometry* 35, 69–89.
- Ibarra, J.B., Muñoz, E., Moliner, R., 1996. FTIR study of the evolution of coal structure during the coalification process. *Organic Geochemistry* 24, 725–735.



- Iglesias, M.J., Jiménez, A., Laggoun-Défarge, F., Suárez-Ruiz, I., 1995. FTIR Study of Pure Vitreous and Associated Coals. *Energy & Fuels* 9, 458–466.
- Kara-Gülbay, R., Korkmaz, S., Yaylalı-Abanuz, G., Erdoğan, M.S., 2018. Organic Geochemistry and Depositional Environment of the Oltu Gemstone (Coal) in the Erzurum Area, NE Anatolia, Turkey. *Energy Fuels* 32, 1451–1463.
- Korte, C., Hesselbo, S.P., 2011. Shallow marine carbon and oxygen isotope and elemental records indicate icehouse-greenhouse cycles during the Early Jurassic. *Paleoceanography* 26 PA4219. <https://doi.org/10.1029/2011PA002160>.
- Mänd, K., Muehlenbachs, K., McKellar, R.C., Wolfe, A.P., Konhauser, K.O., 2018. Distinct origins for Rovno and Baltic ambers: Evidence from carbon and hydrogen stable isotopes. *Palaeogeography, Palaeoclimatology, Palaeoecology* 505, 265–273.
- Mastalerz, M., Schimmelmann, A., 2002. Isotopically exchangeable organic hydrogen in coal relates to thermal maturity and maceral composition. *Organic Geochemistry* 33, 921–931.
- Penton S. (2008). Cumwhitton, Cumbria: analytical investigation of jet-like objects from a Viking cemetery: archaeological conservation report. *English Heritage 2008; Historic England Research Reports*. p 9. <https://doi.org/10.5284/1033757>.
- Pollard, A.M., Bussell, G.D., Baird, D.C., 1981. The analytical investigation of early Bronze age jet and jet-like material from the Devizes Museum. *Archaeometry* 23, 139–167.
- R Core Team, 2023. R: A language and environment for statistical computing. R Foundation for Statistical Computing, Vienna, Austria. URL: <https://www.R-project.org/>.
- A. R. Facsády. (2009): Aquincumi ékszerek. Jewellery in Aquincum. Budapest. (Az Aquincumi Múzeum gyűjteménye 1; The collection of the Aquincum Museum 1).
- Redding, C.E., Schoell, M., Monin, J.C., Durand, B., 1980. Hydrogen and carbon isotopic composition of coals and kerogens. *Physics and Chemistry of the Earth* 12, 711–723.
- Schimmelmann, A., Lewan, M.D., Wintsch, R.P., 1999. D/H isotope ratios of kerogen, bitumen, oil, and water in hydrous pyrolysis of source rocks containing kerogen types I, II, IIS, and III. *Geochimica Et Cosmochimica Acta* 63, 3751–3766.
- Sheridan, J.A., Davis, M., 1995. The Poltalloch “jet” spacer plate necklace. *The Kist* 24, 1–9.
- Sheridan, A., Davis, M., Clark, I., Redvers-Jones, H., 2002. Investigating jet and jet-like artefacts from prehistoric Scotland: the National Museums of Scotland project. *Antiquity* 7, 812–825.
- Suzuki, R., Shimodaira, H., 2006. Pvcust: an R package for assessing the uncertainty in hierarchical clustering. *Bioinformatics* 22 (12), 1540–1542.
- Teichmüller, M., 1992. Organic petrology in the service of archaeology. *International Journal of Coal Geology* 20, 1–21.
- Thomas J.T. (2014): Emerging economies : late Neolithic and Copper Age beads and pendants of the Portuguese Estremadura. PhD (Doctor of Philosophy) Thesis, University of Iowa, 2014, pp. 291.
- To, T.Q., Shah, K., Tremain, P., Simmons, B.A., Moghtaderi, B., Atkin, R., 2017. Treatment of lignite and thermal coal with low cost amino acid based ionic liquid-water mixtures. *Fuel* 202, 296–306.
- Wassenaar, L.I., Hobson, K.A., Sisti, L., 2015. An online temperature-controlled vacuum-equilibration preparation system for the measurement of  $\delta^2\text{H}$  values of non-exchangeable-H and of  $\delta^{18}\text{O}$  values in organic materials by isotope-ratio mass spectrometry. *Rapid Commun. Mass Spectrom.* 29, 397–407.
- Watts, S., Pollard, A.M., 1996. Identifying archaeological jet and jet-like artifacts using FTIR. *Infrared and Raman Users Group, Postprints*, pp. 37–52.
- Watts, S., Pollard, A.M., Wolff, G.A., 1997. Kimmeridge jet – a potential new source for British jet. *Archaeometry* 39, 125–143.
- Zhang, W., Jiang, S., Wang, K., Wang, L., Xu, Y., Wu, Z., Shao, H., Wang, Y., Miao, M., 2015. Thermogravimetric Dynamics and FTIR Analysis on Oxidation Properties of Low-Rank Coal at Low and Moderate Temperatures. *International Journal of Coal Preparation and Utilization* 35 (1), 39–50.
- Zieger, L., Littke, R., Hartkopf-Fröder, C., Schwarzbauer, J., 2020. Comparative geochemical and pyrolytic study of coals, associated kerogens, and isolated vitrinites at the limit between subbituminous and bituminous coal. *International Journal of Coal Geology* 227, 103517.